Supplementary Information

Self-assembly of Isolated Plasmonic Dimers with Sub – 5 nm Gaps on a Metallic Mirror†

Vasanthan Devaraj,*[ab] Isaac Azahel Ruiz Alvarado, [c] Jong-Min Lee, [d] Jin-Woo Oh, *[e] Uwe Gerstmann, [c] Wolf Gero Schmidt, [c] and Thomas Zentgraf *[ab]

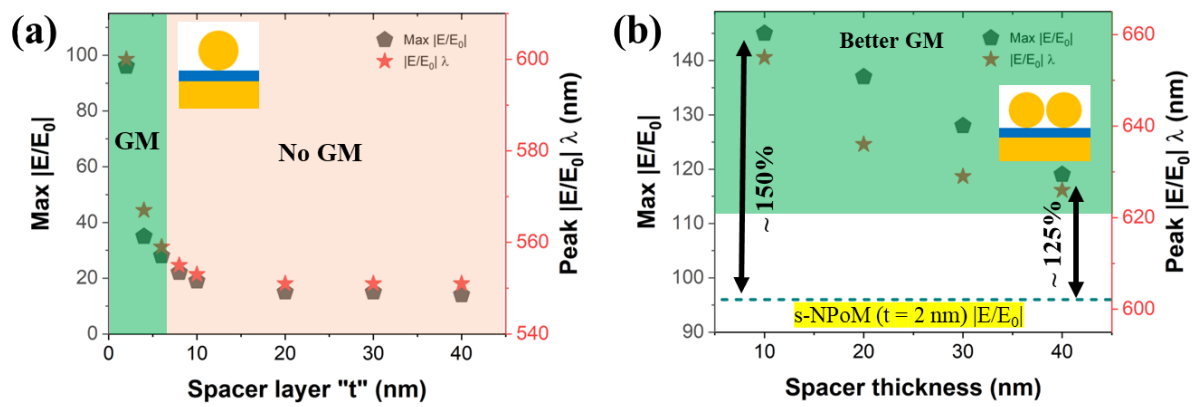

Fig. S1 Simulated near-field spectra for (a) s-NPoMs and (b) d-NPoMs. Maximum near-field intensity $|E/E_0|$ at the peak resonance wavelength "λ" is plotted as a function of varied spacer layer thickness "t". GM denotes gap-plasmonic mode.

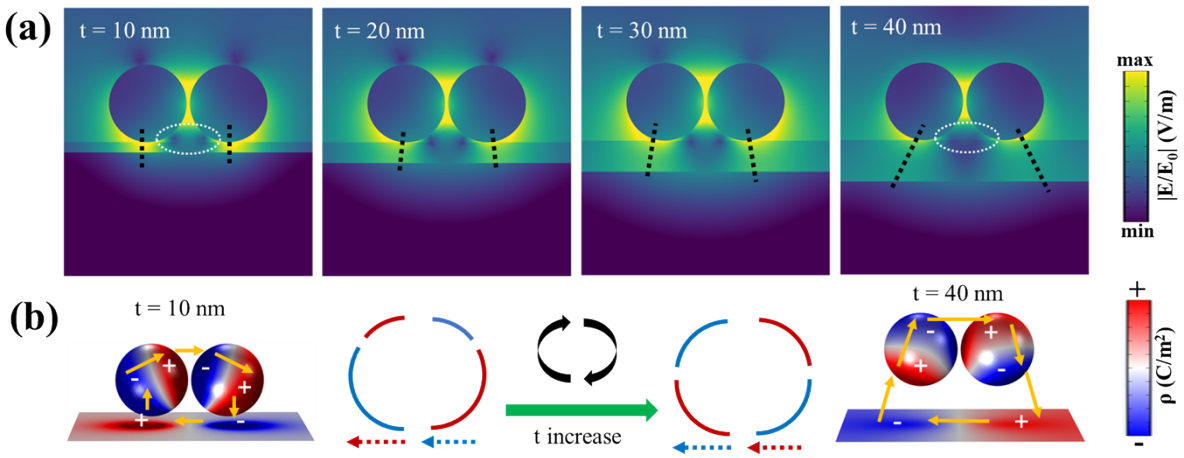

Fig. S2 Properties of d-NPoMs as a function of M13 phage thickness "t". (a) Cross-sectional XZ electric field amplitude profiles with a spacer layer thickness t ranging from 10 nm to 40 nm. The black dotted line indicates the directionality of near-field coupling between the nanoparticle and the metallic mirror. The dotted white ellipse highlights the differences in near-field intensity occurring at the spacer layer interface close to the dimer. (b) Three-dimensional surface charge density distributions as a function of M13 phage thickness "t". The bright dipolar mode remains intact regardless of changes in M13 phage thickness from 10 nm to 40 nm, highlighting a significant advantage of the d-NPoM architecture. The surface charge mapping represents a time-dependent oscillation parameter, where the positions of the signs are not critical; what matters is the dipolar mode.

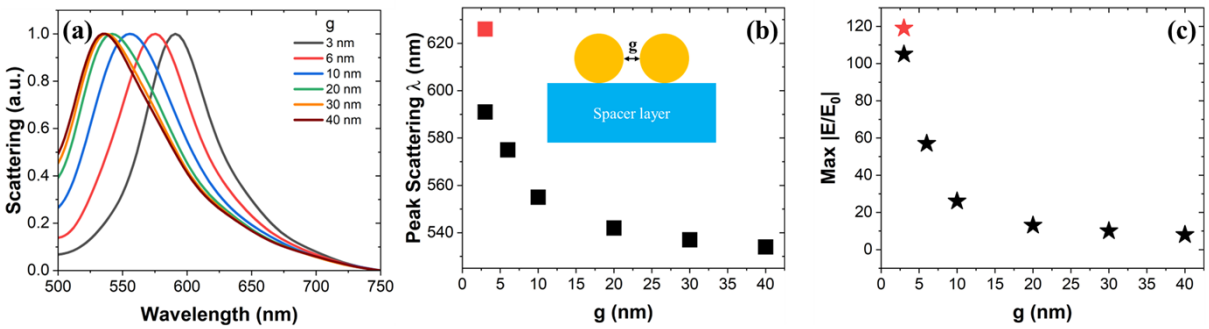

Fig. S3 (a) Simulated plasmonic scattering from dimer NPs without metallic mirror in bottom. The inter-particle distance g is varied. (b) Peak scattering resonances as a function of g for dimer NP on a spacer layer (solid black box) versus d-NPoM with M13 phage thickness of 40 nm (solid red box). (c) Max $|E/E_0|$ as a function of g for dimer NP on a spacer layer (solid black stars) versus d-NPoM with M13 phage thickness of 40 nm (solid red star).

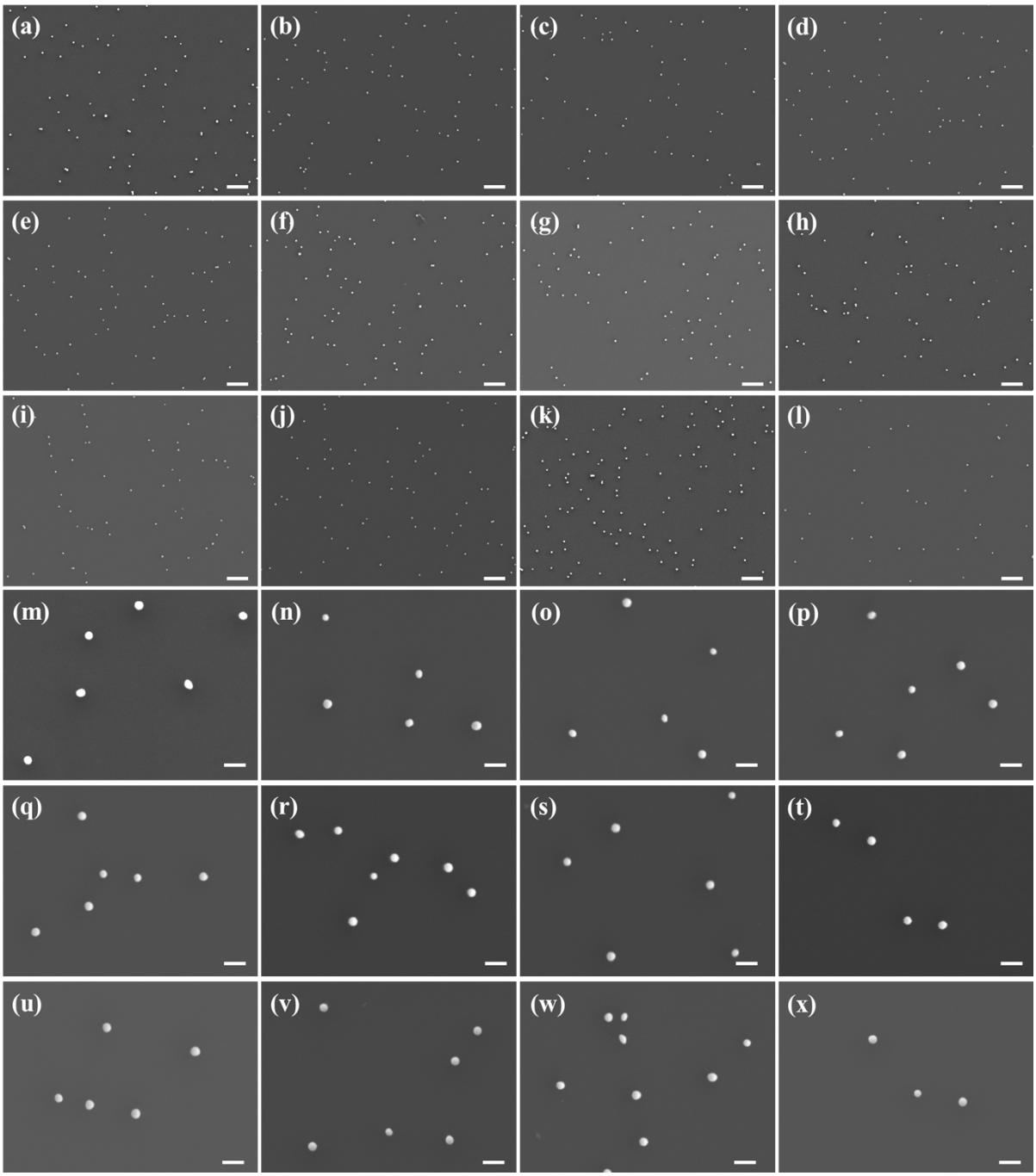

Fig. (S4) SEM images taken from spin-coated Au NPs on a SiO_2/Au substrate. (a – l) These images, taken from different samples, confirm the dominant formation of s-NPoM architectures. Scale bar is 1 µm. Negligible or very few d-NPoMs are formed. (m – x) Closer views of SEM images taken from (a – l), respectively. Scale bar is 200 nm.

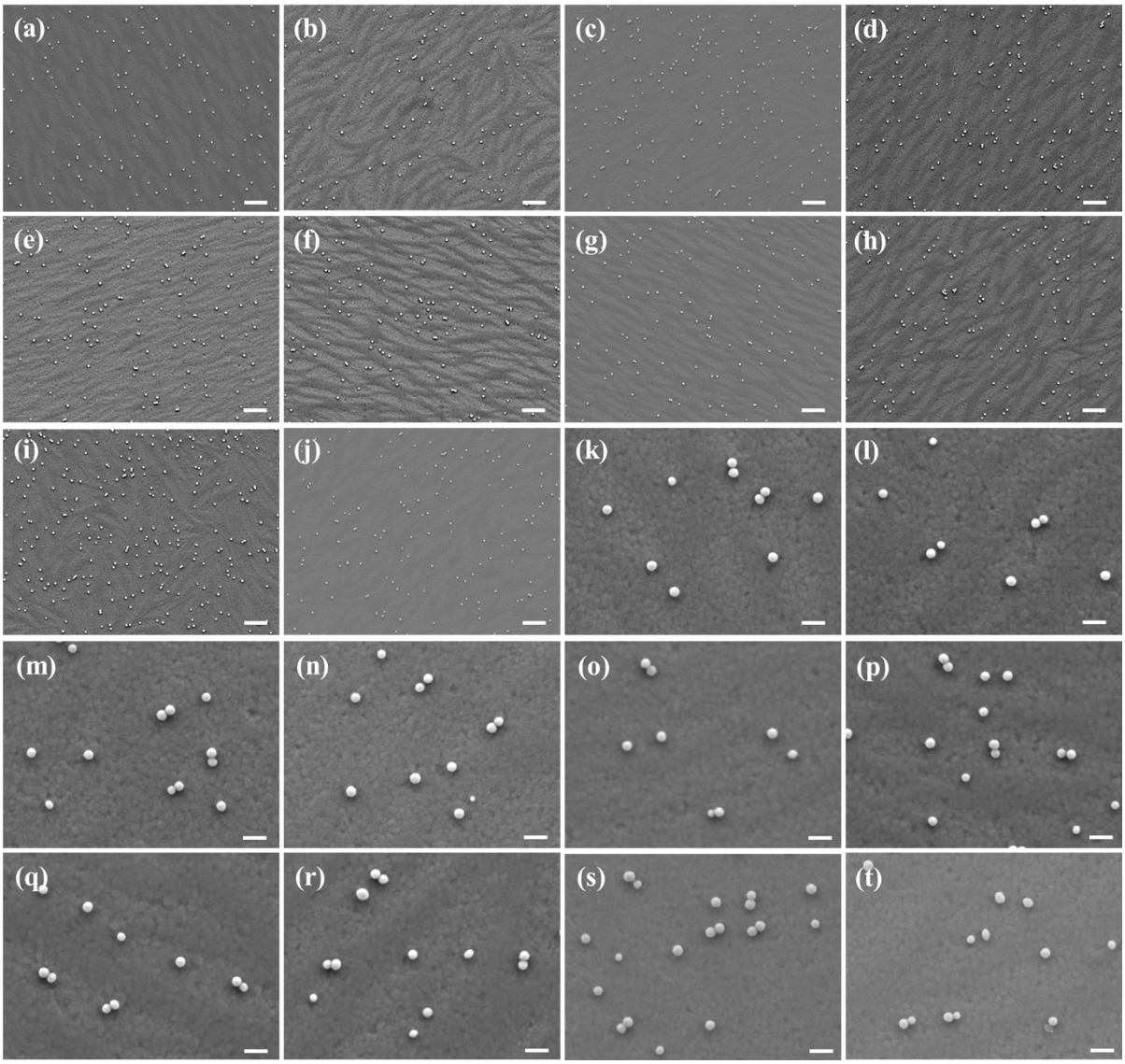

Fig. S5 Reproducibility test. SEM images taken from spin-coated Au NPs on an M13 bacteriophage/Au substrate. (a – j) These images, taken from different samples, confirm the consistent formation of d-NPoM architectures, which are clearly isolated from each other. Scale bar is 1 µm. (k – t) Closer views of SEM images taken from (a – j), respectively. Scale bar is 200 nm. These results confirm the reproducibility of d-NPoMs through our fabrication method.

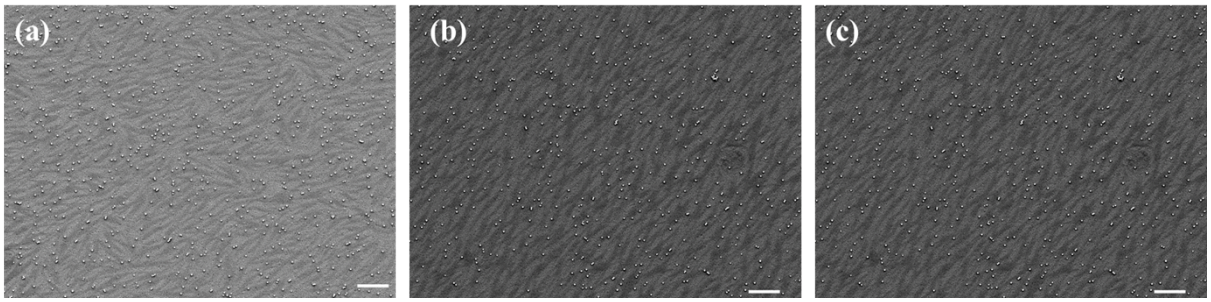

Fig. S6 SEM images (wider area) taken from spin-coated Au NPs on an M13 bacteriophage/Au substrate, confirming the reproducibility of d-NPoMs through our fabrication method. The scale bar is 2 μm.

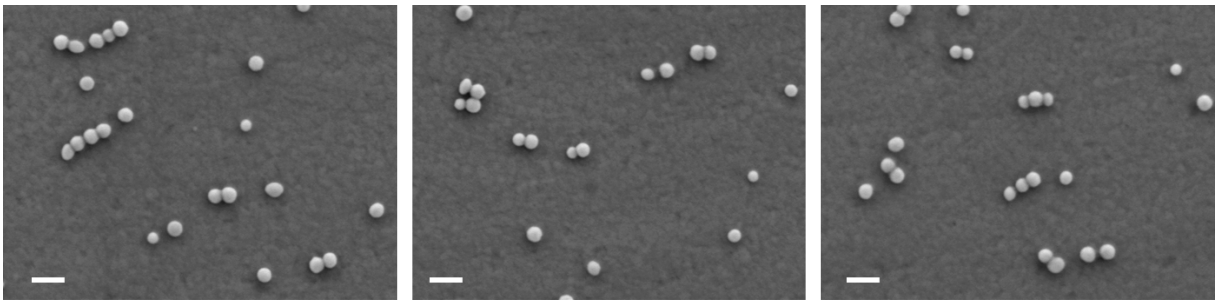

Fig. S7 SEM images of higher-order NP aggregates observed in limited areas of the sample. The scale bar is 100 nm. The formation of these higher-order NP aggregates is extremely negligible compared to the widespread dimer assemblies across the sample.

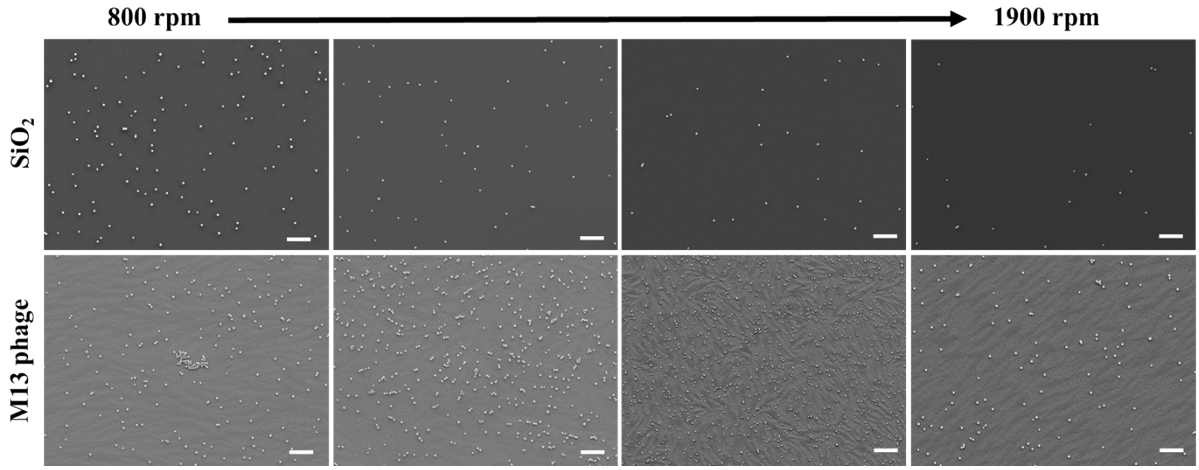

Fig. S8 Spin coating conditions were varied from 800 rpm to 1900 rpm (with a fixed duration of 120 seconds). Top four images show the dominant formation of s-NPoMs on a SiO_2/Au substrate. The bottom four SEM images display the aggregation of NPs or close NP arrangements with particle numbers ≥ 2 on an M13 bacteriophage/Au substrate. These observations support our DFT theory, indicating enhanced free movement/mobility of Au pairs when the M13 phage is involved. Scale bar is 1 µm.

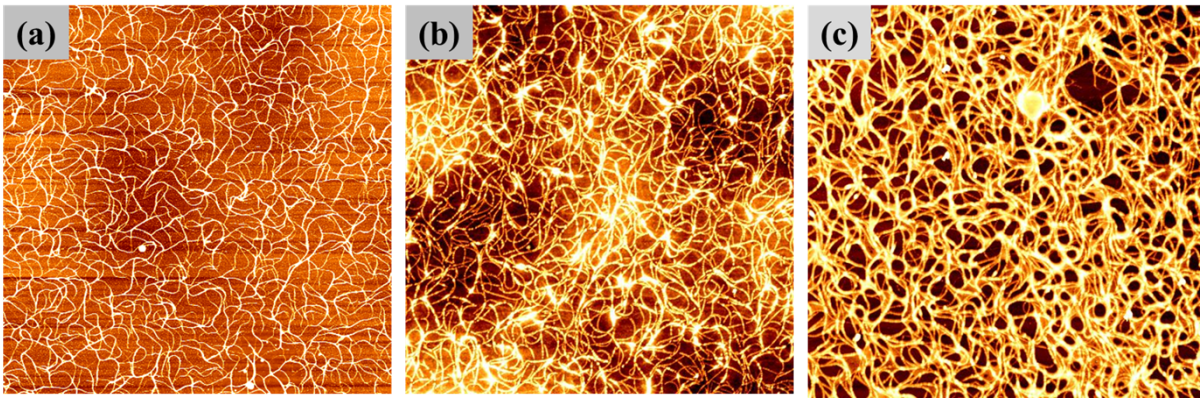

Fig. S9 AFM data from non-continuous M13 phage films attempting to fabricate thicknesses < 10 nm. The M13 phage concentrations used are as follows: (a) 0.1 mg/ml, (b) 1 mg/ml, and (c) 2 mg/ml. The fabricated structures exhibit the formation of single to bundled nanowire geometries and porous structures. The AFM scan area is 10 µm x 10 µm.

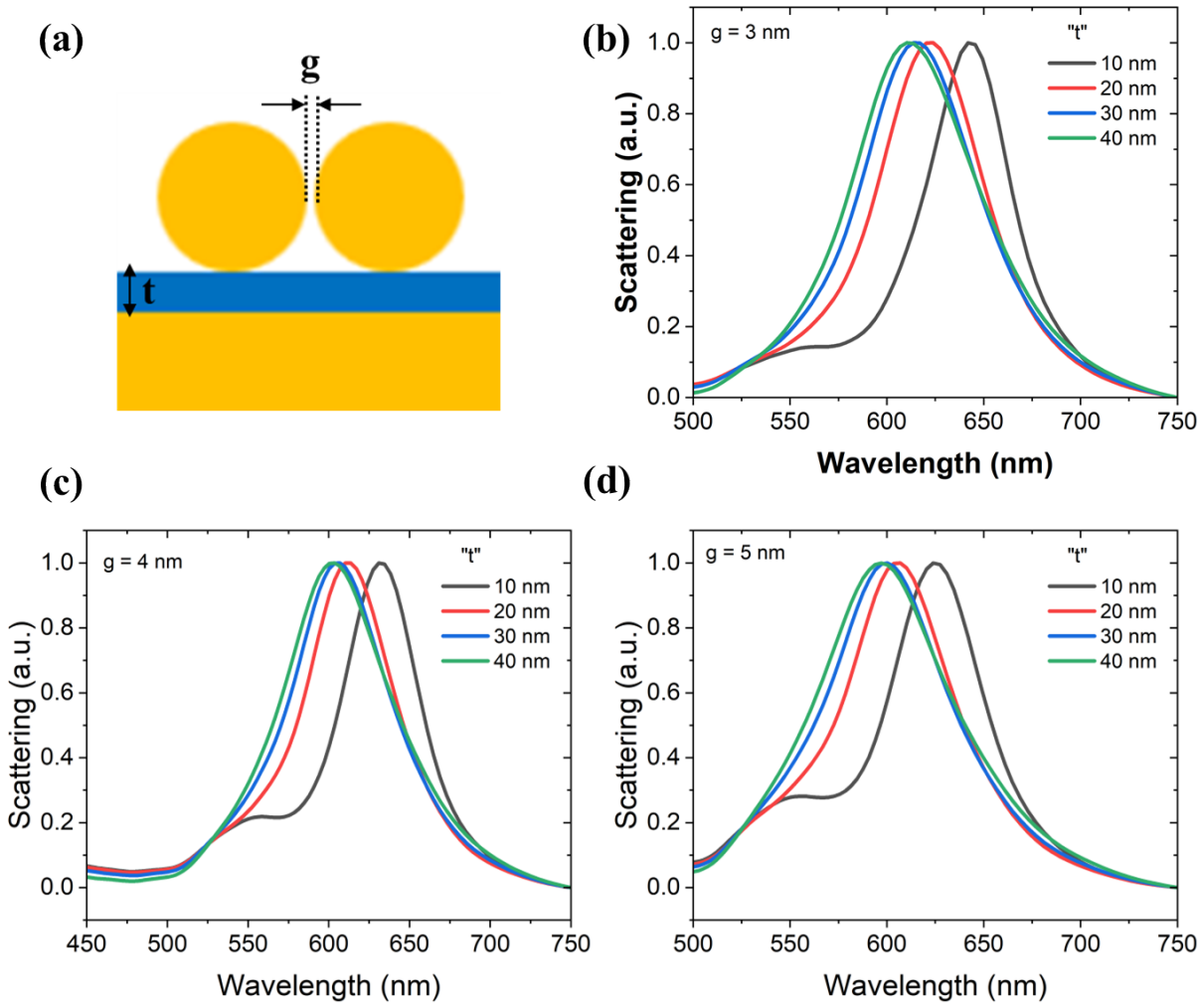

Fig. S10 (a) Plasmonic scattering for d-NPoM model considering the "g" and "t" parameters. Simulated plasmonic scattering for g = 3 nm (b), 4 nm (c), and 5 nm (d) as function of varied "t" ranging from 10 nm – 40 nm.

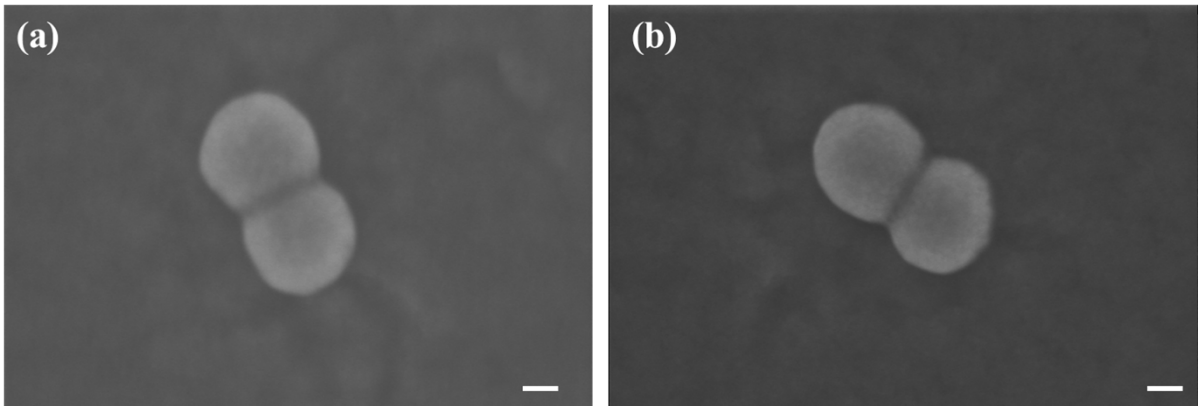

Fig. S11 High-magnification SEM images of d-NPoMs. The estimated interparticle distance between NPs is approximately 5 nm. The scale bar represents 30 nm.

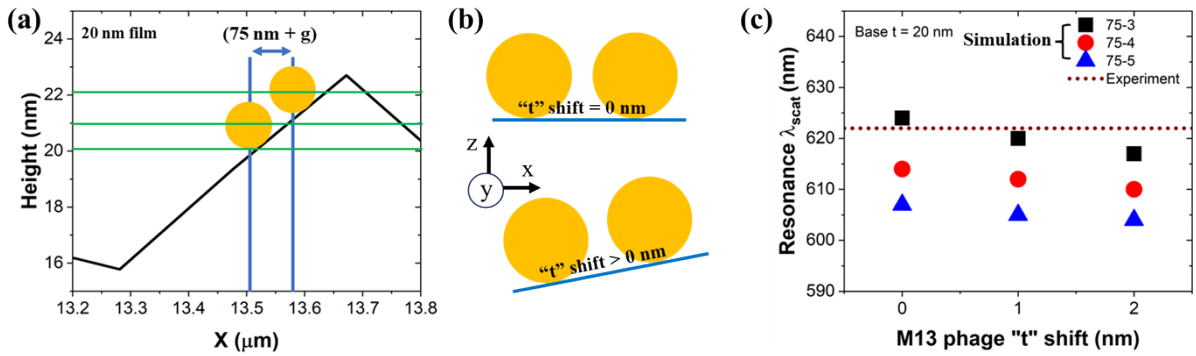

Fig. S12 (a) AFM height profile taken from a 20 nm thick M13 phage film. Considering the NP sizes of 75 nm and the gap 'g,' the inclined height difference is estimated to be approximately 2 nm. (b) Simulations were carried out comparing a flat M13 phage film (t shift = 0 nm) with an inclined film (t shift > 0 nm), where NPs are positioned on uneven heights. (c) Simulated versus experimental peak scattering resonances for the 20 nm thick M13 phage film. The legend (e.g., 75-3) describes an NP with a diameter of 75 nm and a gap size 'g' of 3 nm. Minimal or negligible differences in peak scattering resonance are observed. For M13 phage film thicknesses of 30 nm or 40 nm, the changes in peak scattering resonance are expected to be minimal, with a deteriorating blue shift as seen in Figure 7(h).

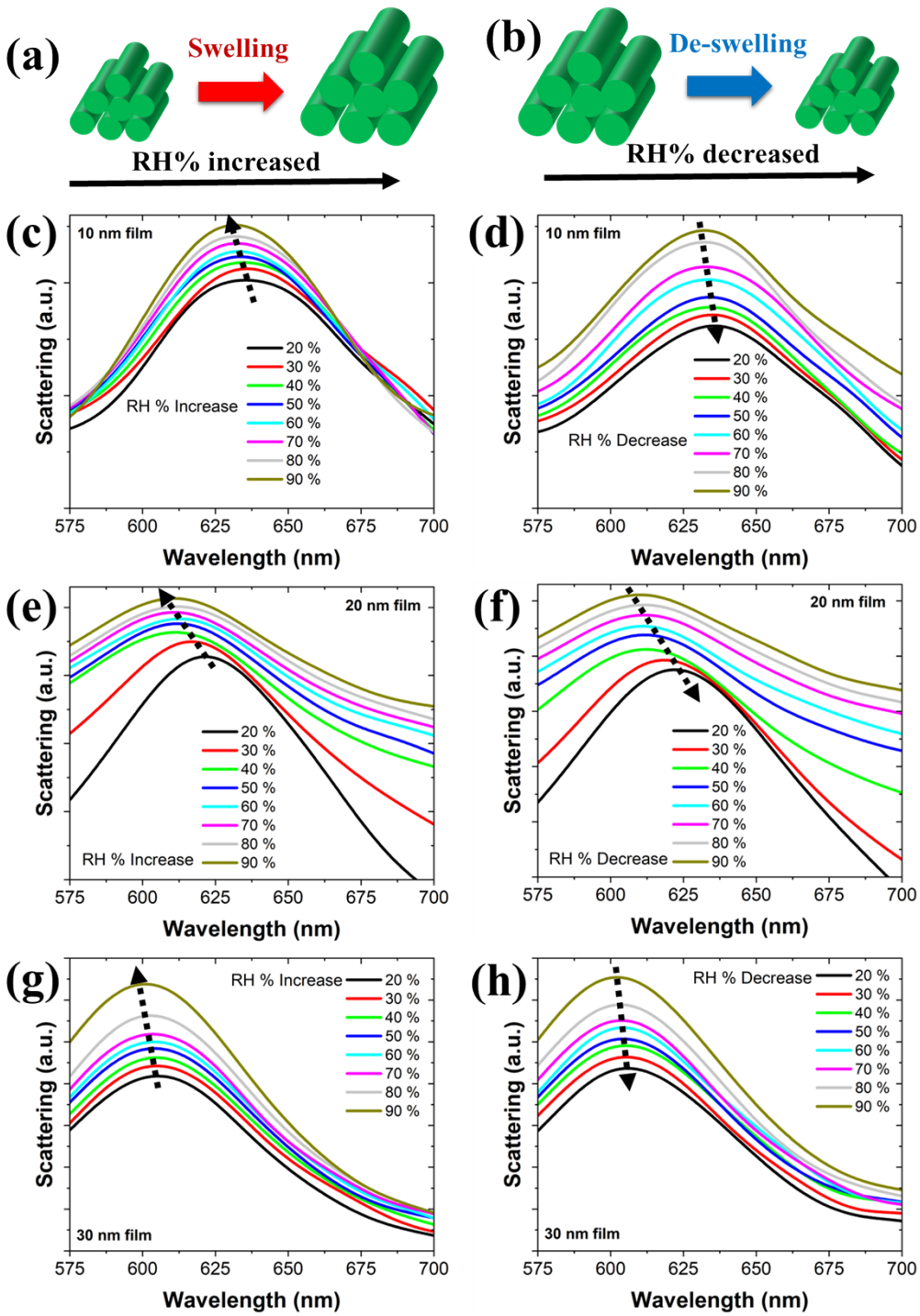

Fig. S13 Relative humidity based experimental scattering spectra. (a, b) Schematic illustration of relative humidity RH % based M13 phage thickness change. Experimental plasmonic scattering data for 10 nm (c, d), 20 nm (e, f), and 30 nm – thick (g, h) M13 phage films in d-NPoM architectures for increasing and decreasing RH %. Scattering spectra are vertically translated to clearly display the scattering wavelength resonance shift (dotted arrows).